SI Appendix for

The structure of a minimum amyloid fibril core formed by necroptosis-mediating RHIM of human RIPK3

Xia-Lian Wu[1,3,6#], Yeyang Ma[2,3#], Kun Zhao[2,3#], Jing Zhang[1,3,6], Yunpeng Sun[2,3], Yichen Li[4,5], Xing-Qi Dong[1,3,6], Hong Hu[1,3,6], Jing Liu[1,3,6], Jian Wang[1], Xia Zhang[1], Bing Li[1], Hua-Yi Wang[1], Dan Li[4,5], Bo Sun[1], Jun-Xia Lu[1*], Cong Liu[2,3*]

[1]School of Life Science and Technology, ShanghaiTech University, Shanghai, 201210, China

[2]Interdisciplinary Research Center on Biology and Chemistry, Shanghai Institute of Organic Chemistry, Chinese Academy of Sciences, Shanghai 201210, China

[3]University of Chinese Academy of Sciences, Beijing 100049, China

[4]Bio-X-Renji Hospital Research Center, Renji Hospital, School of Medicine, Shanghai Jiao Tong University, Shanghai, 200240, China

[5]Bio-X Institutes, Key Laboratory for the Genetics of Developmental and Neuropsychiatric Disorders, Ministry of Education, Shanghai Jiao Tong University, Shanghai, 200030, China

[6]State Key Laboratory of Molecular Biology, CAS Center for Excellence in Molecular Cell Science, Shanghai Institute of Biochemistry and Cell Biology, Chinese Academy of Sciences, Shanghai 200031, P. R. China

#These authors contributed equally to this work.

*Correspondence: J-X. L. (lujx@shanghaitech.edu.cn); C. L. (liulab@sioc.ac.cn)

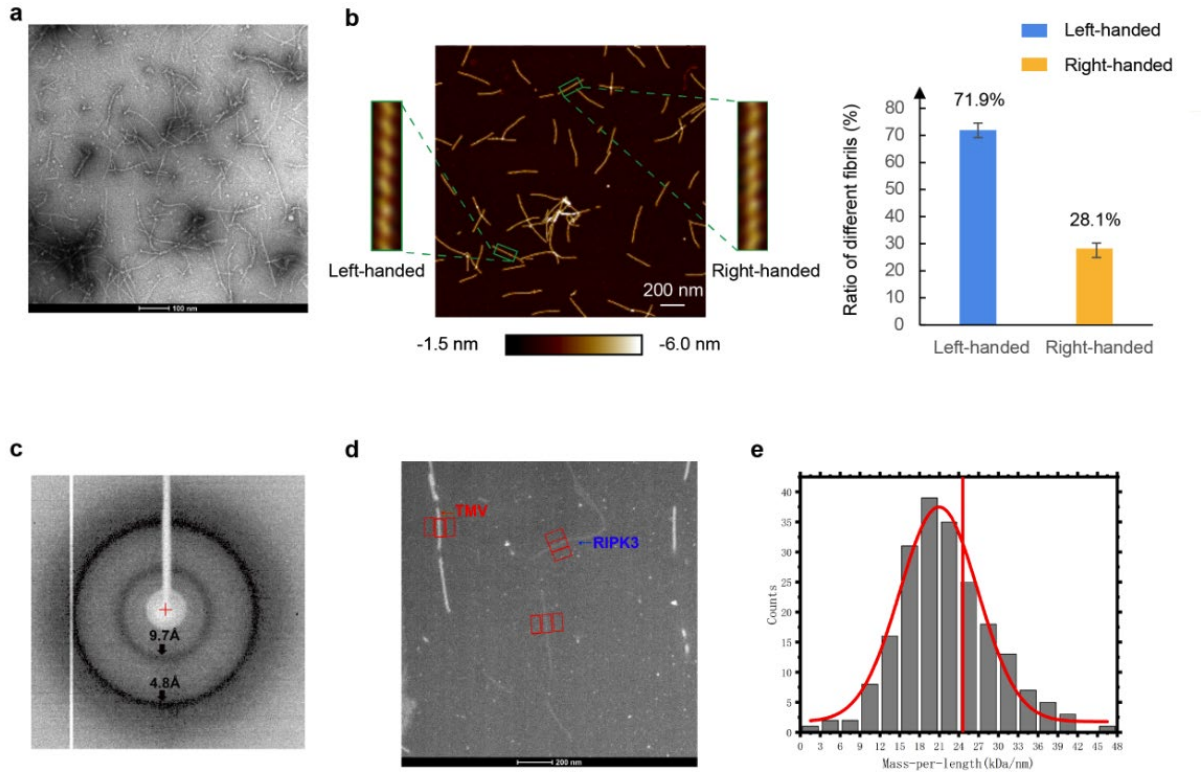

Fig. S1. a, A representative EM image of human RIPK3-CTD$_{NMR}$ fibrils. **b**, AFM measurement of RIPK3-CTD$_{NMR}$ fibril. An AFM 2D image and zoom-in views of fibrils with different handedness are shown. The populations of RIPK3-CTD$_{NMR}$ fibrils in left- and right-handedness were calculated based on AFM measurements. Data shown are mean ± s.d., n=3 images. **c**, X-ray diffraction image of human RIPK3-CTD$_{NMR}$ fibrils. The arrows indicated equatorial and meridional reflection at about 9.7Å and 4.8Å resolutions, respectively. **d**, One BT-TEM image of RIPK3-CTD$_{NMR}$ fibrils (blue arrow), with tobacco mosaic virus (TMV) particles (red arrow) as the standard for MPL measurement. **e**, MPL histogram of RIPK3 fibrils derived from BT-TEM images indicates only one monomer in a cross subunit of fibrils, where the red line shows the theoretical value.

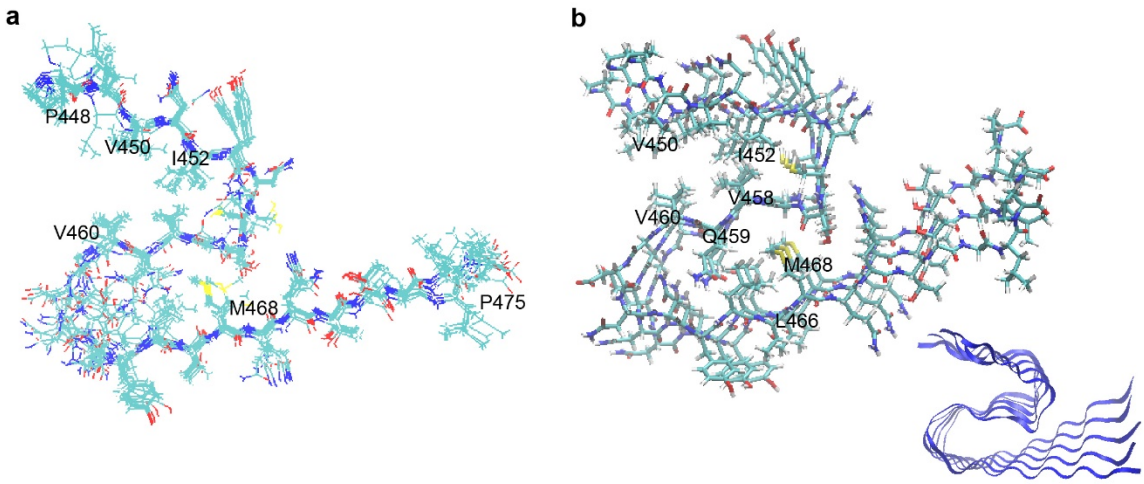

Fig. S2. The RIPK3-CTD$_{NMR}$ fibril structure calculated from NMR restraints. a, Superimposed 12 structures with the lowest energy in the monomer form. Residues from V450 to M468 are mostly aligned while the two loop regions show different side-chain orientations. **b**, A fibril core structure showing 3 layers of fibril. A ribbon representation of 5 layers of fibril was also shown in inset. The summary of restraints was shown in table S3.

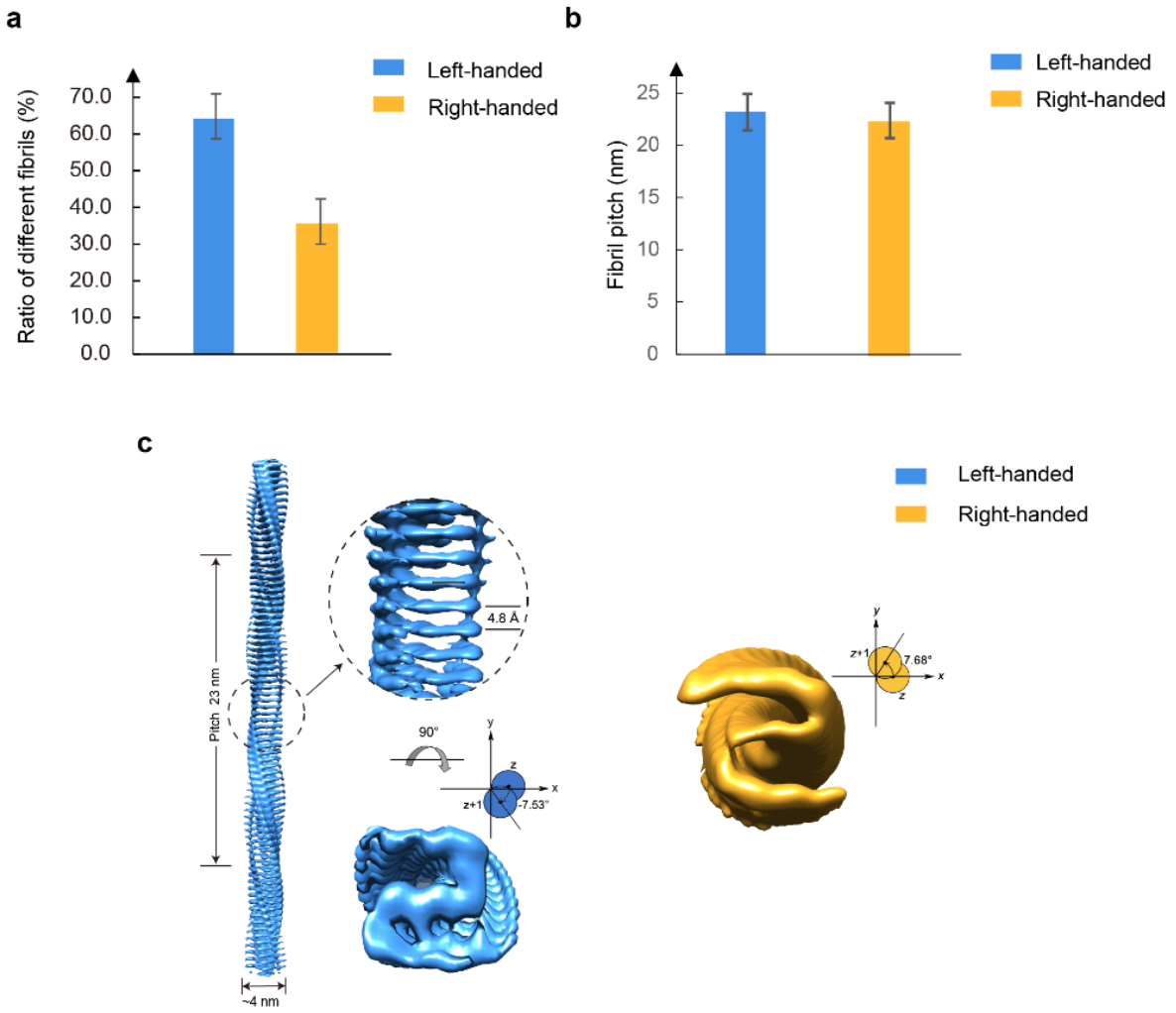

Fig. S3. AFM analysis and cryo-EM reconstruction of RIPK3-CTD$_{EM}$ fibrils with different handedness. a, The population of RIPK3-CTD$_{EM}$ fibrils in left- and right-handedness was calculated based on AFM measurements. Data shown are mean ± s.d., n=3 images. **b**, Fibril pitch of left- and right-handed fibrils. AFM images were used for data analysis. Data shown are mean ± s.d., n=15 individual fibrils from 3 images. **c**, Cryo-EM reconstruction density maps of left- and right-handedness fibrils are shown. Fibril width and pitch length are indicated. The twist angle is graphically illustrated. Graphing was performed with UCSF Chimera v1.13.

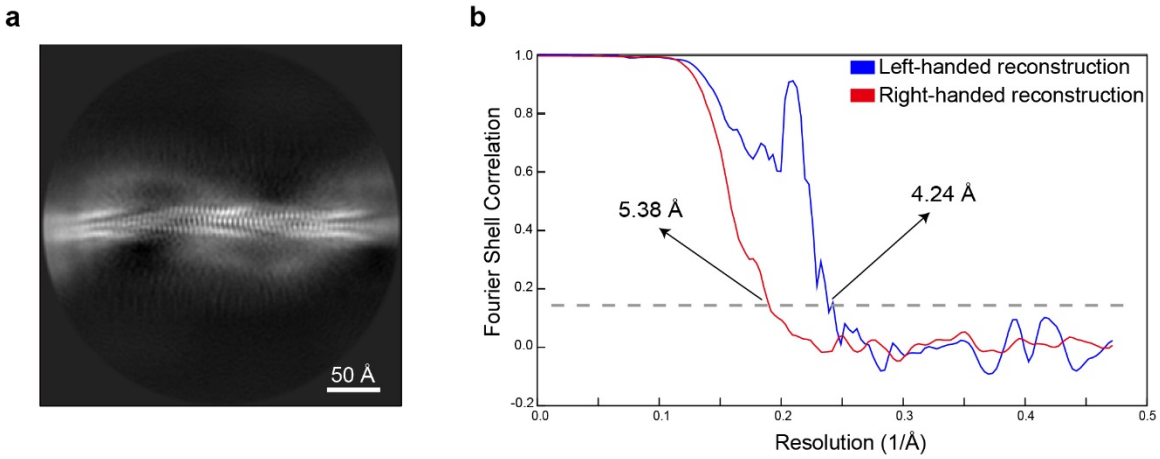

Fig. S4. 2D class averages and resolution estimation of RIPK3-CTD$_{EM}$ fibril. a, Representative 2D classification image of RIPK3-CTD$_{EM}$ fibril. **b**, Gold-standard Fourier shell correlation curves of RIPK3-CTD$_{EM}$ fibrils with different handedness. The overall resolution of the left-handed reconstruction is 4.24 Å and the overall resolution of the right-handed reconstruction is 5.38 Å.

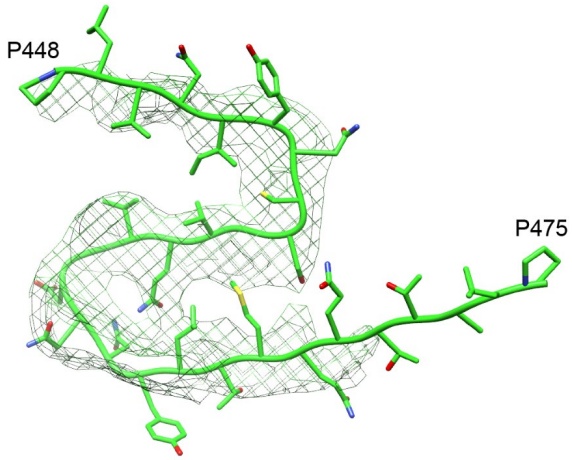

Fig. S5. Comparison of the RIPK3-CTD fibril structures determined by ssNMR and cryo-EM. RIPK3-CTD structure model derived from ssNMR data is fitted into cryo-EM density map.

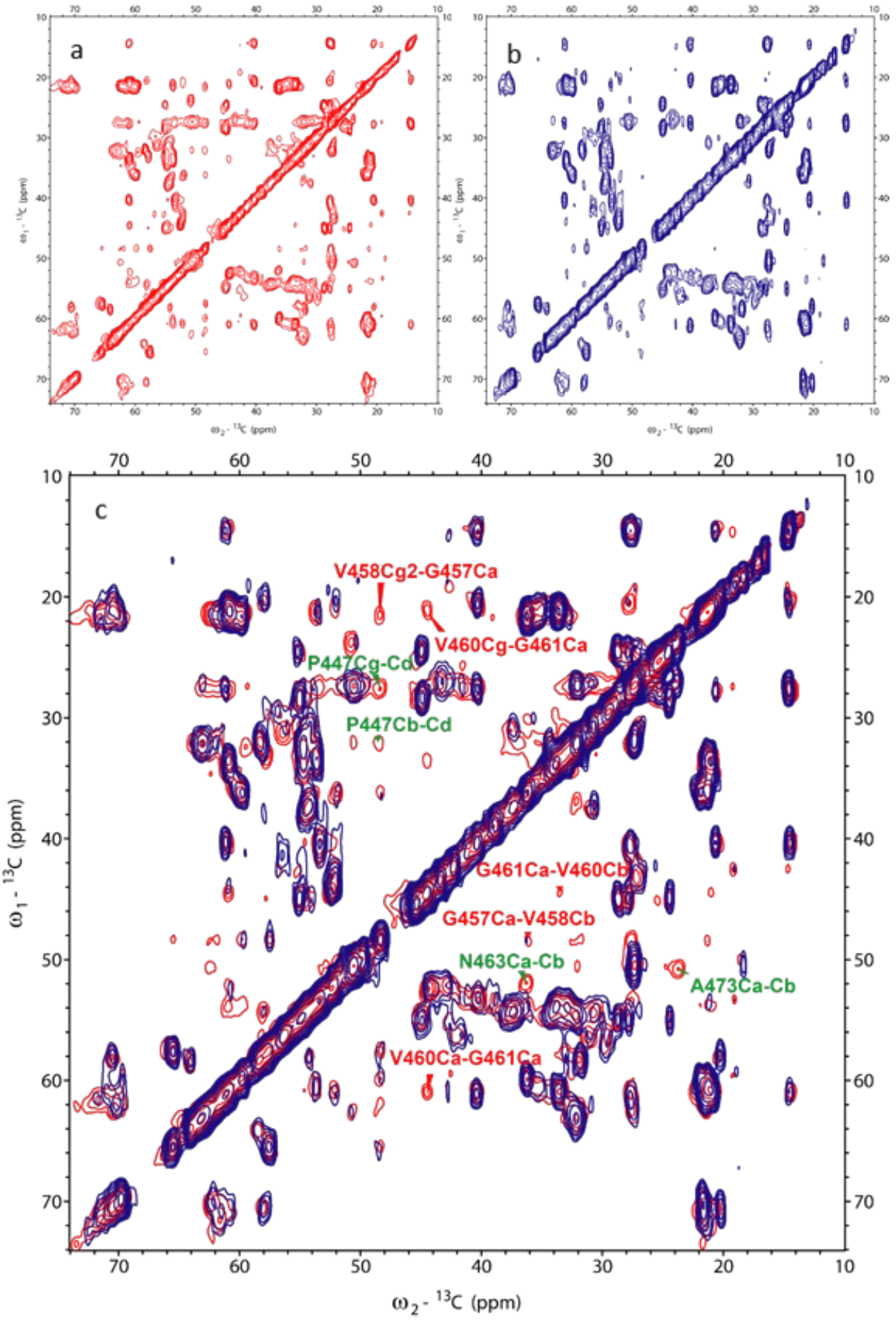
a
b
c
V458Cg2-G457Ca
V460Cg-G461Ca
P447Cg-Cd
P447Cb-Cd
G461Ca-V460Cb
G457Ca-V458Cb
N463Ca-Cb
A473Ca-Cb
V460Ca-G461Ca
ω1 - 13C (ppm)
ω2 - 13C (ppm)

Fig. S6 Comparison between the 2D ^{13}C-^{13}C ssNMR spectra of RIPK3-CTD$_{NMR}$ fibrils and RIPK3-CTD$_{EM}$ fibrils using 50 ms DARR mixing. a, 2D ^{13}C-^{13}C spectrum of uniformly [^{13}C/^{15}N]-labeled RIPK3-CTD$_{NMR}$ fibrils (red). **b**, 2D ^{13}C-^{13}C spectrum of uniformly [^{13}C/^{15}N]-labeled RIPK3-CTD$_{EM}$ fibrils (blue). **c**, 2D ^{13}C-^{13}C spectra overlay for RIPK3-CTD$_{NMR}$ fibrils and RIPK3-CTD$_{EM}$ fibrils. The peaks overlay well, which indicates the two samples have similar core structures. The RIPK3-CTD$_{NMR}$ fibrils have extra peaks, mainly from three intra-residue peaks P447C γ -Cδ, N463Cα-Cβ, and A473Cα-Cβ in green, consistent with the solid-state NMR structure. Other inter-residue peaks labeled in red from V457Cα-G458Cα, V457Cα-G458Cβ, V458Cγ2-G457Cα, V460Cα-G461Cα, V460Cγ-G461Cα are also visible for RIPK3-CTD$_{NMR}$ fibrils using 50 ms DARR mixing.

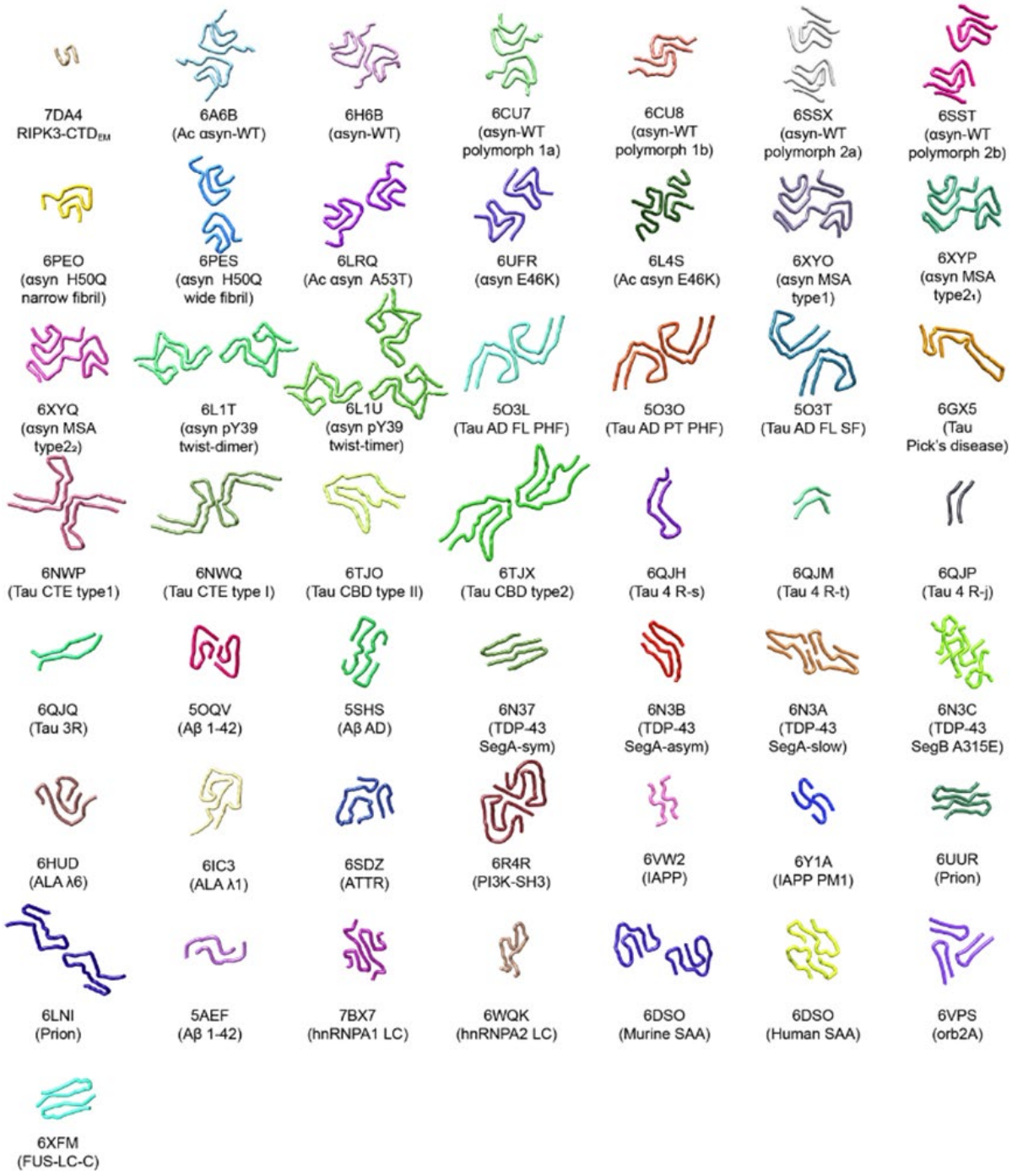

Fig. S7. Cryo-EM structure models of different amyloid fibrils. 50 cryo-EM fibril structures are shown in different colors. The RIPK3-CTD fibril exhibits the smallest fibril core. PDB IDs and protein information are provided below each structure model. All structures are shown in ribbons.

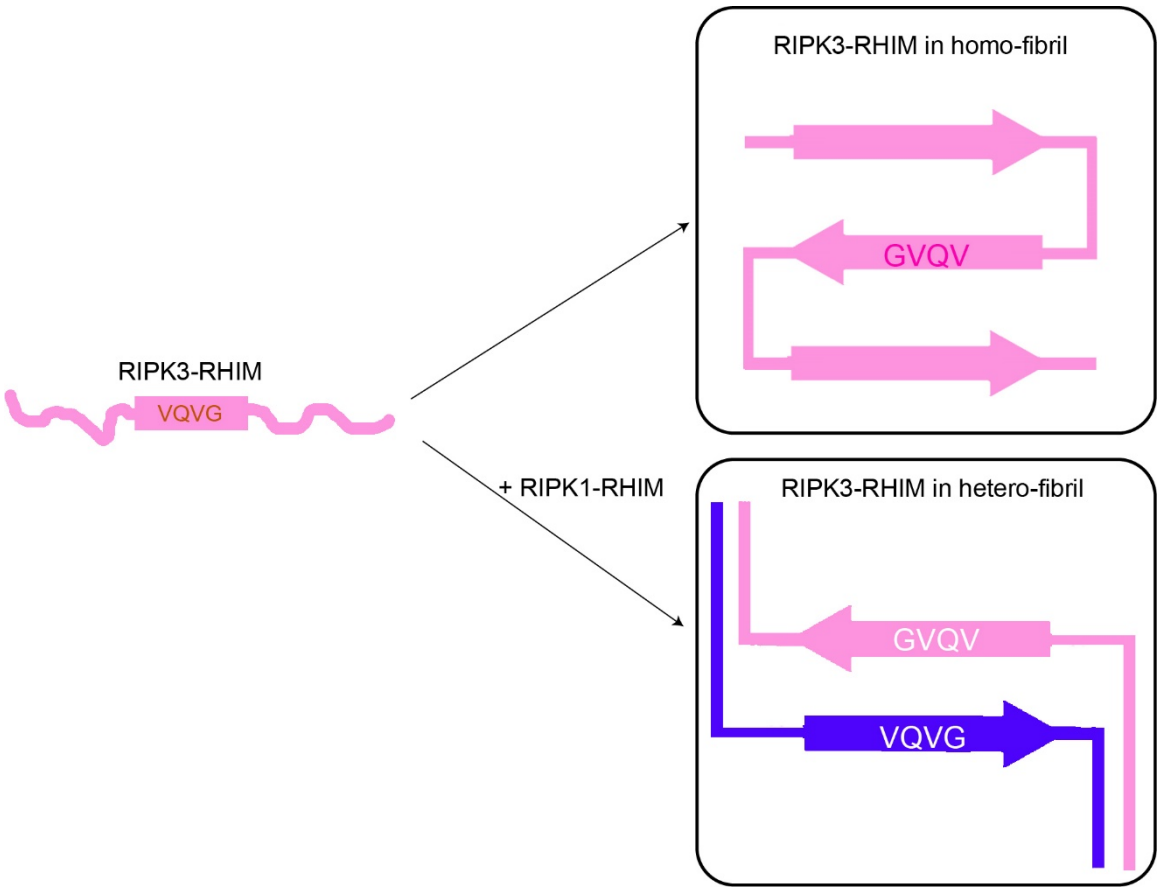

Fig. S8. Schematic diagram of the different structures of RIPK3 RHIM in the homo- and hetero-fibrils. RIPK3-CTD forms a conserved S-shaped structure with the RHIM domain in the homo-fibril. In contrast, RIPK3-CTD forms a serpentine structure with the RHIM domain in the hetero-fibril in complex with RIPK1-CTD. The VQVG motif plays an essential role in forming both fibrils.

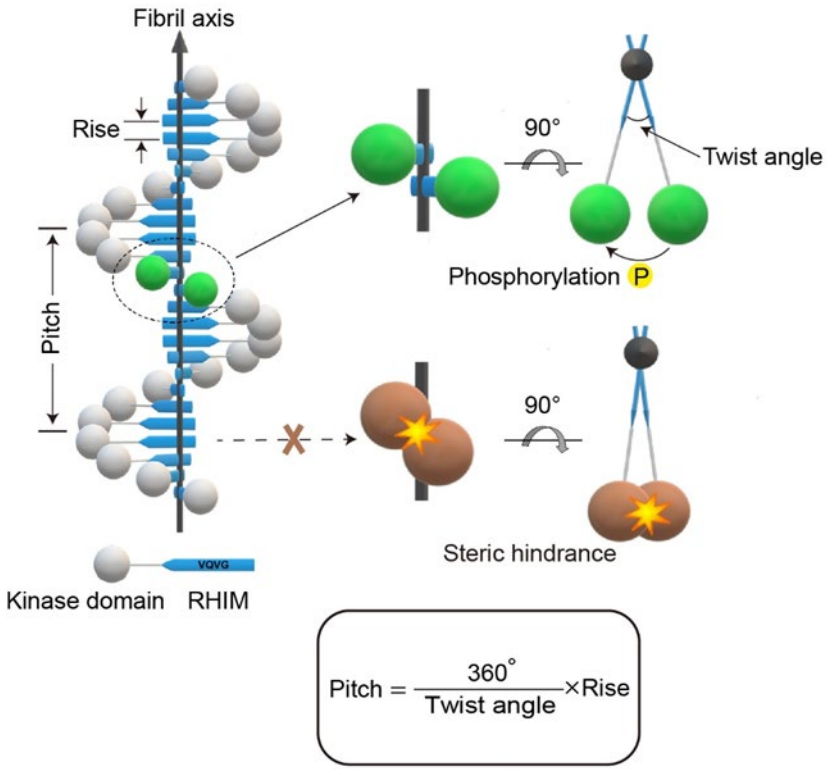

Fig. S9 Schematic diagram of the relationship between fibril pitch, twist angle, and the spatial arrangement of the kinase domain of RIPK3. Large twist angle may provide enough space to arrange the kinase domain outside fibril core for phosphorylation. While, small twist angle may lead to steric hindrance and clash of neighboring kinase domains. The equation describes the relationship between fibril pitch, twist angle and rise.

Table S1. Chemical shift statistics from solid state NMR spectra of human RIPK3-CTD$_{NMR}$ fibrils.

Residue	Chemical shifts (ppm)										
	N	CO	CA	CB	CG/CG1	CG2	CD/CD1	CD2/ND2	CE/CE1	CE2/NE2	CZ
R447				30.8	27.1		43.3				159.6
P448			62.7	32.1	27.4		50.4				
L449					26.5		23.7				
V450		173.9	60.7	34.9	21.2						
N451	124.4	173.6	52.2	42.7	176.3						
I452	122.4	173.9	61.0	40.3	20.5	27.7	14.4				
Y453	123.6	56.2									
N454	121.6	172.1	53.6	41.5	179.8						
C455	112.9	174.3	58.2	32.0							
S456	116.7	173.2	57.6	65.6							
G457	115.2	170.3	48.4								
V458	123.2	174.3	60.0	35.2	21.8	21.3					
Q459	123.3	175.1	54.6	33.4	34.1		179.4			110.6	
V460	123.1	174.4	60.8	33.6	21.1						
G461	115.9	170.3	44.5								
D462	117.9	175.5	52.4	44.4	181.0						
N463	112.7	174.0	52.0	36.3	177.9			111.5			
N464	115.2	173.8	53.4	40.3	176.5			108.7			
Y465	120.5		56.7								
L466	133.5	174.9	54.9	44.8	28.7		24.5				
T467	119.6	172.7	58.1	70.8	20.5						
M468	123.8	174.6	54.5	34.2	32.3				16.9		
Q469	123.3	174.9	54.5	30.8	37.5		179.5				
Q470	122.0	175.9	53.8	33.8	36.4		177.8				
T471	115.9	172.2	61.6	71.5	21.5						
T472	125.7	172.5	62.3	70.4	21.4						
A473	128.8	175.6	50.7	23.7							
L474	121.7	173.9	55.0	45.3	27.6		25.3				
P475	135.0	175.8	62.2	32.2	27.6		48.4				

Table S2. Restraints used in RIPK3-CTD$_{NMR}$ fibril structural calculation with Xplor-NIH.

Xplor-NIH potential term										
CDIH									NOE	
torsion angles based on 'strong' prediction by TALOS-N (all errors were expanded as described in the method)						parallel cross-β sheet (intermolecular alignment) (Å)			long-range contacts (residue crosspeaks)	
									unambiguous	low Ambiguity
resid	Ψ	Φ	ΔΨ	ΔΦ	χ(Δχ)	C-C	H_n-O_{n-1}	N_n-O_{n-1}	inter-residue	residues
									DARR	DARR
									(5.5±1.5Å)	(5.5±2.5Å)
R447									I452Cd1-Q459Ca,	N451C-V450Cg#/V460Cg#,
P448									S456Cb-V458Ca/Cg#,	N451Cg-V450Cg#/V460Cg#,
L449					-58.7(8.6)				S456Ca-V458Ca,	N451Cb-V450Cg#/V460Cg#,
V450	136.1	-113.3	35.0	35.0	-176.2(6.4)				S456Cb-M468Cg/Ce,	I452Cd1-V458Cg#/V460Cg#,
N451	140.6	-120.8	37.5	40.6					S456Ca-M468Ce,	I452Cg1-G457C/G461C,
I452	130.6	-115.0	43.5	20.0	-56.5(8.8)	4.75±0.1	2.3±0.1	3.3±0.1	S456C-M468Ce,	S456Cb-V458Cb/Q470Cg,
Y453	142.4	-123.5	47.3	46.8	-61.1(9.5)				G457Ca-N454C/Ca/Cb,	Q459Cd-D462Ca/N463Ca,
N454	151.8	-102.6	35.0	77	-64.1(11.0)				G457Ca-M468Cg/Ce,	V460Cg#-N451Ca/D462Ca/N463Ca,
C455	160.4	-148.0	35.0	49.3					G457C-M468Ce,	D462Ca-G461Ca/N463Cb,
S456									G457C-L466Cg,	N463Cb-G461Ca/D462Cb,
G457						4.75±0.1			V458Cg#-N454C,	N464Cb-Q459Cg/V460Cb,
V458	147.1	-126.4	39.6	35.0	-174.5(8.5)				Q459Cd-G461Ca,	L466Cg-Q459Cb/V460Cb,
Q459	138.7	-124.5	43.1	45.6			2.3±0.1	3.3±0.1	V460Ca/Cb/Cg#-D462Cg,	L466Cd2-Q459Cb/V460Cb
V460	168.8	-102.4	52.2	40.0	-172.7(10.2)		2.3±0.1	3.3±0.1	G461C-N463Cg,	
G461									D462Cg-N464Cg,	
D462	159.5		47.5							
N463										
N464					-63.5(8.7)					
Y465	127.6	-101.1	41.3	57.3						
L466	128.8	-110.3	35.0	35.0	179.1(6.5)	4.75±0.1				
T467	131.6	-114.6	35.0	35.0	59.3(11.5)		2.3±0.1	3.3±0.1		
M468	128.0	-110.9	35.0	45.6						
Q469	133.7	-103.9	36.7	44.1			2.3±0.1	3.3±0.1		
Q470	144.4	-129.3	36.3	35.0						
T471	129.3	-110.0	35.0	49.9	-56.5(14.0)		2.3±0.1	3.3±0.1		
T472	129.1	-101.9	35.0	35.0	-58.6(5.9)					
A473	141.6	-125.9	39.9	35.0						
L474	148.7	-118.9	40.9	71.5	-63.8(6.7)					

Table S3. Summary of NMR restraints for xplor-NIH calculations of human RIPK3-CTD$_{NMR}$ fibrils.

constraints	number
dihedral angles	38
chi angles	13
unambiguous intramolecular residues contacts	79 (22 non-sequential)
ambiguous intramolecular residues contacts	13
intermolecular constraints	parallel beta-sheet

PDB ID 7DAC

BMRB ID 36392

Table S4. Statistics of cryo-EM data collection and structure refinement.

Name	**RIPK3-CTD$_{EM}$ fibril (Left-handed)**	**RIPK3-CTD$_{EM}$ fibril (Right-handed)**
PDB ID	7DA4	
EMDB ID	EMD-30622	
Data Collection		
Magnification	22,500	22,500
Pixel size (Å)	0.53	0.53
Defocus Range (μm)	-2.3 to -1.3	-2.3 to -1.3
Voltage (kV)	300	300
Camera	K3	K3
Microscope	Titan Krios	Titan Krios
Exposure time (s/frame)	0.097	0.097
Number of frames	32	32
Total dose (e^-/Å)	55	55
Reconstruction		
Micrographs	3,460	3,460
Manually picked fibrils	15,505	15,505
Box size (pixel)	288	288
Inter-box distance (Å)	33.92	33.92
Segments extracted	904,654	904,654
Segments after Class2D	294,736	294,736
Segments after Class3D	45,526	37,016
Resolution (Å)	4.24	5.38

Map sharpening B-factor (Å^2)	-271.84	-359.53
Helical rise (Å)	4.80	4.80
Helical twist (°)	-7.53	7.64
Atomic model		
Non-hydrogen atoms	507	
Protein residues	66	
Ligands	0	
r.m.s.d. Bond lengths	0.010	
r.m.s.d. Bond angles	1.542	
All-atom clashscore	77.78	
Rotamer outliers	0.00%	
Ramachandran Outliers	0.00%	
Ramachandran Allowed	50.00%	
Ramachandran Favored	50.00%	